Analytical Modeling of the Stretching in the Bimetallic Materials Produced by Equal Channel Angular Pressing

A. M. Rashidi[1]*, M. Etemadi[2]

[1] Department of Materials Science and Textile Engineering, Razi University, Kermanshah, Iran
[2] Department of Mechanical Engineering, Langarud Branch, Islamic Azad University, Langarud, Iran

ABSTRACT: The main idea of the present work is to provide an analytical approach for the analysis of mating surface stretch during successive equal channel angular pressing of core/shell bimetallic materials. Furthermore, the novel relationships between maximum stretches induced in each equal channel angular pressing pass with the numbers of passes and the yield strength of equal channel angular pressed steel/ copper bimetallic are presented. To evaluate established relations, the tensile test is performed on steel cores of the copper/steel bimetallic samples subjected to consecutive equal channel angular pressing process up to three passes with route BC, which rotates the samples by +90 º around the longitudinal axis between each equal channel angular pressing pass. The results indicated that, for a given equal channel angular pressing die, the maximum stretch is a linear function of pass number of deformation with equal channel angular pressing process. The values of the angular position corresponding to extreme values of stretch increased as the number of pass deformations with route BC increased. Also, the value of the minimum stretch could be increased beyond a threshold value in an equal channel angular pressing process with route B by increasing the number of pass deformation. After N passes deformation by the equal channel angular pressing process, the yield strength of bimetallic samples can also be determined by estimating the maximum stretch using an established predictive model.

1- Introduction

Recently, the Equal-Channel Angular Pressing (ECAP) of bimetallic materials is regarded as one of the most effective ways to improve the quality of cold welding between two dissimilar metals, which leads to increasing interfacial bonding strength [1-13]. For example, Eivani and Taheri [1] indicated that the interfacial bonding strength of copper clad aluminum subjected to two passes of Equal Channel Angular Extrusion (ECAE) was 12.5% higher than those of samples produced by the general extrusion process. According to results reported by Ghadimi et al. [2], the shear bonding strength between Al and Cu in bimetallic tubes produced by ECAP was increased from 4.2 MPa for the first pass to 5.9 MPa after three passes. The ECAP of bimetallic materials improves the bonding strength and simultaneously results in exceptional grain refinement to the submicrometer or nanometer level, resulting in high strength and unique properties of bimetallic materials that are not typically observed in conventional coarse-grained and mildly deformed materials [3].

The surface stretch is defined as the distance ratio between the two presumed points before and after deformation per initial distance [4]. It plays an important role in cold welding by ECAP process between bimetallic core/shell materials

constituents during their Severe Plastic Deformation (SPD). The cold welding mechanism in the ECAE process of bimetallic materials has been well discussed by Zebardast and Karimi Taheri [4]. As a result, a cold weld between the sheath and core is generated by surface stretching cracking the work-hardened layer of the mating surfaces, then penetrating metal into the produced cavities, extruding it through the cracks, and finally reaching the distance between two metals to an atomic distance, resulting in a solid metallurgical bonding. This mechanism has been previously proposed for solid-phase welding in the rolling deformation process [13-17]. Based on the proposed mechanism, the surface stretch produced by the ECAE process during severe plastic deformation of bimetallic materials is a key parameter affecting the formation of cracks on the interface, so it is essential to reach the surface stretch to a threshold value to create surface cracks [4].

Moreover, the formation of a wavy interface between constituents of core/shell bimetallic materials leads to a superior debonding resistance [18], greater toughness of fracture [19], and higher joint strength of welding [20], in comparison with the straight interface. In the previous work, we showed that induced stretch by the ECAP process plays an important role in forming a wavy interface of the bimetallic material [21]. Therefore, its analytical modeling is essential.

The relationship between the induced stretch by ECAP

*Corresponding author's email: rashidi1347@razi.ac.ir

Table 1. The composition of the used low carbon steel rod and copper tube [21].

Steel rod	Element	C	Mn	Si	P	S		Ni	Cr	Fe
	wt%	0.105	0.439	0.105	0.014	0.01		0.032	0.01	balance
Copper tube	Element	Cu	Pb	Fe	Si	Other				
	wt%	> 99.9	0.033	0.016	0.016	< 0.025				

with the shear strain (γ) and angular displacements (rotation angular around the longitudinal axis of the sample, θ) was formulated in Ref. [4]. However, the presented model for the surface stretch has a major limitation addressed in this study. The model is designed on the one sample passing through the die; in practice, however, the sample should be pressed repetitively through the die to attain exceptionally high strains, resulting in ultra-fine grained or nanocrystalline microstructure [22, 23]. It is well known that the quality of the bimetallic interface is improved as the number of ECAP passes increases [24]. In the previous work [21], the induced shear strain during the first, second, and third passes of the ECAP process with route Bc was modeled and used to calculate the induced mating surface stretch amounts at different points of copper/steel bimetallic interface. However, the presented approach for the calculation of surface stretches has some limitations. It lacks a mathematical formula to derive the answer directly. Also, estimating the surface stretch introduced through the various routes of repetitive passing deformation has yet remained. It is impossible to choose one route over the other as a suitable route for producing bimetallic samples unless the surface stretch formed by one can be distinguished from the other. In the present study, we tried to overcome these problems by presenting a novel and simple mathematical formula to account for the surface stretch introduced by the repetitive passing deformation with routes of A (without any rotation), B (rotation by ±90° between consecutive passes), and C (rotation by 180° between each passes). Also, a new general relationship between the yield strength (σ_y) of bimetallic materials and the maximum surface stretch (St_{max}) has been extracted and evaluated. This approach would benefit the researcher to estimate the yield strength of bimetallic samples after several passes of deformation by the ECAP process.

2- Materials and Procedures

In order to evaluate the established relation between σ_y and St_{max}, the bimetallic rods were prepared by inserting the low carbon steel rods inside copper tubes with an inner diameter of 8mm and an outer diameter of 9.5 mm. The composition of the used constituents is presented in Table 1. Then, the work-pieces with 100 mm length were undergone a severe plastic deformation via passing through an ECAP

solid die having a die inner angle of ϕ=90° and an outer curvature corner angle of ψ=30°, internal surfaces plated with a MoS_2 lubricant. The ECAP process was performed at room temperature (298 K) using a hydraulic press operating with a 20 mm/min ram speed. Al samples were processed up to three passes with route Bc (+90° clockwise rotation around the sample axis between each pass), as shown in Fig. 1. More details of the applied ECAP process can be found in Ref [21]. In order to measure the yield strength of steel cores, the copper shells of ECAPed bimetallic samples were removed by turning. Then, according to the ASTM-E8M standard, small tensile specimens of a steel core with a diameter of 5 mm were prepared. The gauge length and other dimensions of tensile samples are given in Fig. 2. The tensile tests were performed on the prepared samples using a universal testing machine SANTAM -STM-250 at room temperature and a constant strain rate of 10^{-3} s^{-1}. The testing machine's applied tensile force and the corresponding gauge length change were recorded. The engineering stress and strain of the specimens were calculated by dividing the tensile force by the original area of the cross-section of the sample and dividing the gauge length change by the initial gauge length. Then, the engineering stress-strain curves were plotted using the obtained data.

3- Analytical Modeling of the Stretch

In line with the previous study [21], we consider the position of two presumed points A and B on the outer surface of a cylindrical sample with the radius of r before and after deformation by ECAP process according to the state 1 and 2 in Figs. 3a and 3b, respectively. Also, we assumed that the angular positions of these points could be expressed by $\grave{e}_i$ and $\theta_i + \delta\theta$, respectively(Fig. 3c). The induced surface stretch is determined as [4]:

$$St = 100 \times (d_i - d_0)/d_0 \qquad (1)$$

Where $d_0 = r \times \delta\theta$ and d_i are the distance between A and B before and after the i th passing the sample through the die of ECAP deformation.

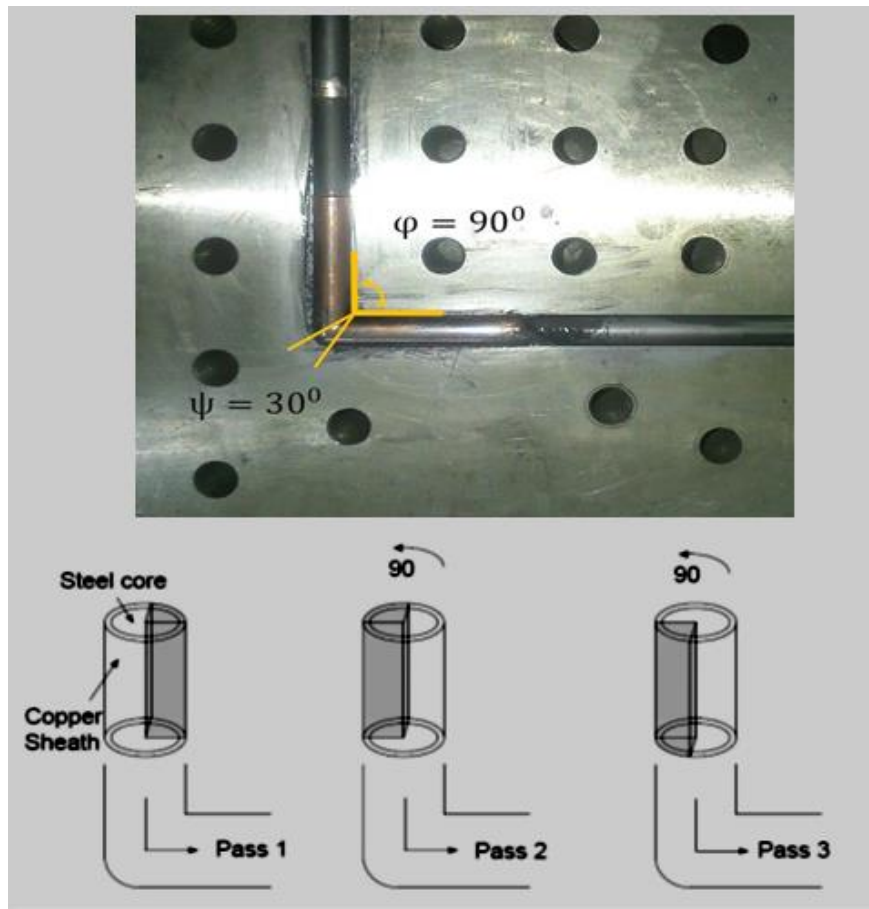The produced shear strain after one pass deformation

Fig. 1. The image of die cross-section with the specimen in the channel (up) and schematic of the sample passage with Bc route (bottom).
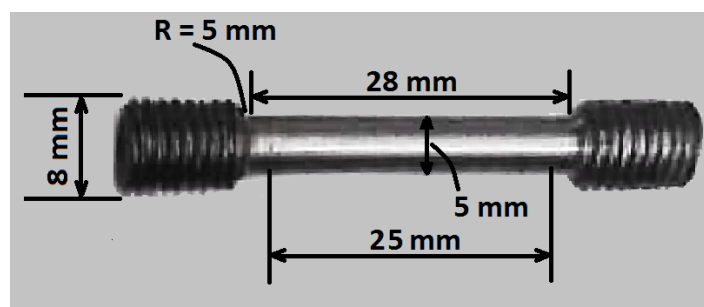

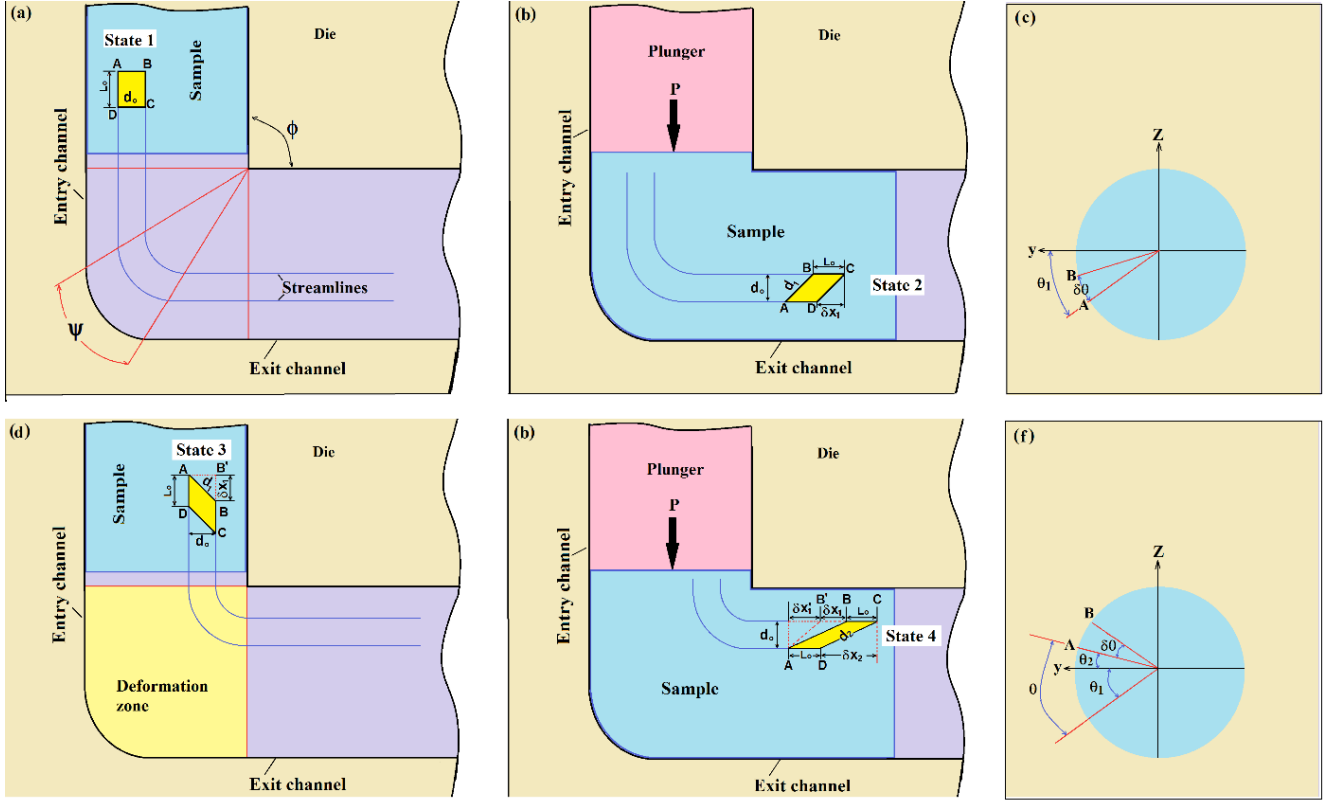**Fig. 2. Presentation of the tensile sample and its dimensions**

Fig. 3. Schematic illustration of ECAP showing the corner arcs of die (and), and the position of two adjacent points A and B in entry (a, d) and exit channels (b, e) and their angular positions (c, f) before and after rotation of sample by around its longitudinal axis.

at the angular position of the θ_1, $(\gamma\theta_1)$ is equal to $\gamma\cos\theta_1$ [4], where the γ (the magnitude of accumulative shear strain induced into the sample in one pass deformation by ECAP die with inner and outer corner angles of ϕ and ψ), is expressed as [25]:

$$\gamma = 2\cot(\phi+\psi)/2 + \psi.\cos ec(\phi+\psi)/2 \tag{2}$$

If at the beginning of the first pass, the angular position of point A and its distance from point B are denoted by, θ_1 and d_1, respectively, then considering the state 2 in Fig. 3b, it can be written:

$$\delta x_1 = d_0\,\gamma\,|\cos\theta_1| \tag{3}$$

$$d_1 = \sqrt{\delta x_1^2 + d_0^2} = d_0\sqrt{(\gamma|\cos\theta_1|)^2 + 1} \tag{4}$$

Now, we consider the general ECAP route, in which the sample is rotated by θ around its longitudinal axis(Fig. 3f) after each pass, then the sample is re-entered into the die input channel, and the ECAP process is performed on it again. At the start of any new pass, the distance of point A from point B (for example the state 3 in Fig. 3d) was the same at the end of the previous pass (state 2 in Fig. 3b). Considering states 3 and 4 in Figs. 3d and 3e, for the second pass, it can be written:

$$d_2 = \sqrt{\delta x_1^2 + d_0^2} = \sqrt{d_0^2 + (\delta x_1 + \delta x_1')^2} = d_0\sqrt{1 + \gamma^2(|\cos\theta_1| + |\cos\theta_2|)^2} \tag{5}$$

At the start of any new pass, the angular position of point A, (θ_i) and its distance from point B, (d_i) differs from the previous one. In the same way, as described above, it can be established that after the Nth passing the sample through the die of ECAP, the distance between two points A and B (d_N) is equal to:

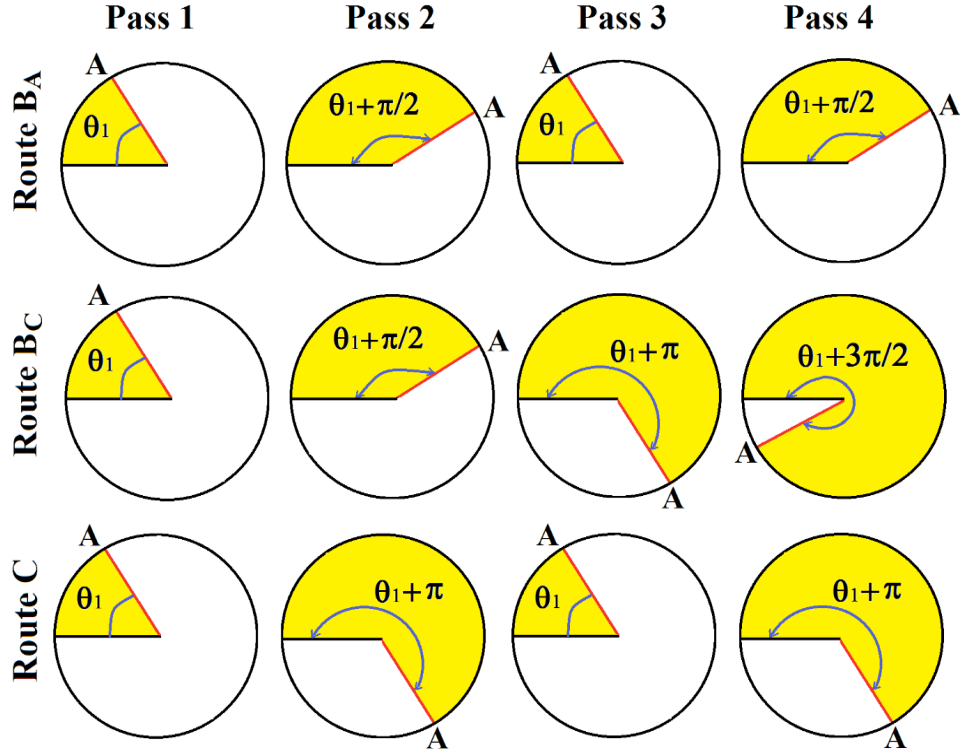$$d_N = \sqrt{d_0^2 + \delta x_N^2} = d_0\sqrt{1 + (f\gamma)^2} \tag{6}$$

Fig. 4. Representation of the angular position of a presumed point A on the cross-section of the sample before first, second, third, and fourth ECAP deformation with routes BA, BC, and C.

Where $f = \sum_{i=1}^{N} |\cos\theta_i|$ is the coefficient of shear strain, N is the number of repeated deformation passes, θ_i is the angular position of any presumed point A in the interface of bimetallic core-shell, which is equal to $\theta_1 + (N-1)\theta$ after the Nth passing of the sample through the die of ECAP. The θ_1 and θ are the angular position of point A before ECAP deformation and the angle of rotation of the specimen around its longitudinal axis between two consecutive passes, respectively.

By substituting the Eq. (6) in for d_i in the first equation, the amount of imposed stretch after Nth passing the sample through the die of ECAP with any route can be formulated as:

$$St_N = 100 \times (\sqrt{1 + (f\gamma)^2} - 1) \tag{7}$$

In Eq. (7), the factor of f is dependent on the applied deformation route and the number of repeated deformation passes (N), as shown in the following.

We consider the known repetitive passing deformation with routes of A, B_A, B_C and C. The angular position of point A is equal to θ_1 for all passes deformation with route A, namely $\theta_{i=2,3..} = \theta_1$, because the sample is not rotated between consecutive passes deformations($\theta = 0$). Therefore,

the factor of f is equal to $N\cos\theta_1$, and the Eq. (7) can be rewritten as:

$$St_{NA} = 100 \times (\sqrt{1 + (N\gamma\cos\theta_1)^2} - 1) \tag{8}$$

The angular positions of a presumed point A are shown in Fig. 4 for ECAP deformation with routes B_A, B_C, and C, before each passes up to four passes of ECAPed samples. This figure indicates that during deformation of the sample by B_A route, the $\theta_i = \theta_1$ when i is odd and $\theta_i = \theta_1 + \frac{\pi}{2}$ when i is even. As a result, the coefficient of shear strain is equal to $f = |\cos\theta_1|_{i=1} + |\sin\theta_1|_{i=2} + |\cos\theta_1|_{i=3} + |\sin\theta_1|_{i=4} + |\cos\theta_1|_{i=5} + ...$. Also, when the ECAP process is carried out with route B_C, the $\theta_i = \theta_1 + (N-1)\frac{\pi}{2}$, as shown in Fig. 4 (second row). As a result, the factor of f^2 becomes the same as that obtained for the B_A route. Based on these results, for both B_A and B_C routes, the coefficient of shear strain can be expressed as:

$$f = \sum_{i=1}^{N} |\cos\theta_i| =$$
$$\frac{1}{2}[N(|\cos\theta_1| + |\sin\theta_1|) +$$
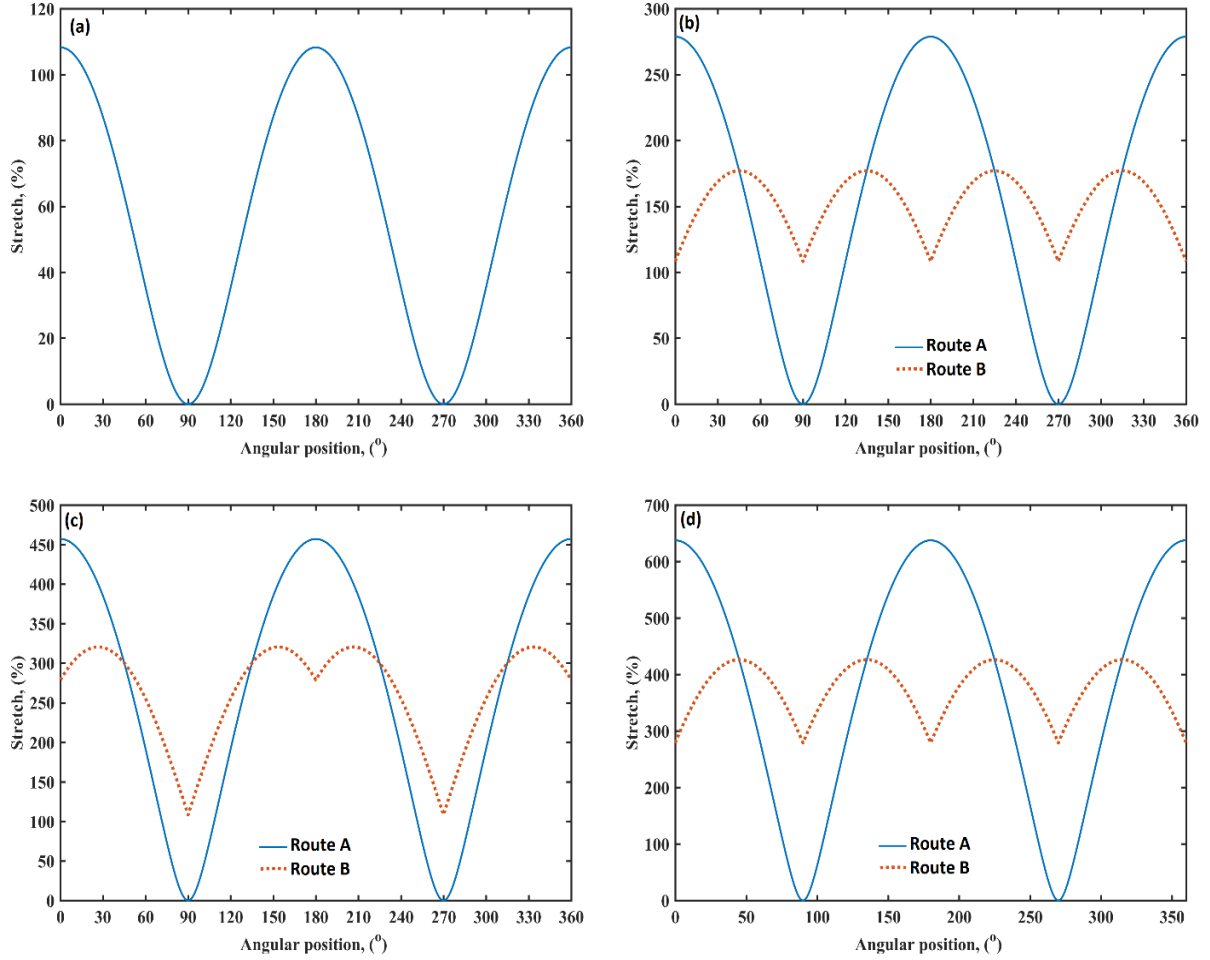$$|\sin N\pi/2|(|\cos\theta_1| - |\sin\theta_1|)] \tag{9}$$

Fig. 5. The variation of stretch with the angular position after a) one, b) two, c) three, and d) four passes of ECAP deformation with routes A and BC (φ=90º and ψ=30º).

The factor $|\sin N \pi / 2|$ is applied to demonstrate the odd-even effect of the pass deformation number (N).

Fig. 4 clearly shows that if the sample deformed by route C, then θ_i is equal to $(N-1)\pi + \theta_1$, and therefore, the f is equal to $\left| \cos \theta_1 \right|_{i=1} + \left| -\cos \theta_1 \right|_{i=2} + \left| \cos \theta_1 \right|_{i=3} + \left| -\cos \theta_1 \right|_{i=4} + \cdots = N \left| \cos \theta_1 \right|$. By substituting the $N \left| \cos \theta_1 \right|$ in Eq. (7), Eq. (8) has already been proven for route A.

4- Results and Discussion

Eq. (7) (after placing Eq. (9)) and Eq. (8) are well revealed the surface stretch-induced during successive passing of bimetallic samples through the die of ECAP. It is convenient to prepare a graphical representation of these equations because this provides a simple visual understanding of the significance of the deformation routes and passes numbers. Therefore, the variation of the imposed stretch after the first, second, third, and fourth passing samples through an ECAP die with ϕ=90º and ψ=30º with angular position (θ) is compared for routes A and B in Fig. 5.

Fig. 5 depicted the distribution of imposed stretch along the angular position is not uniform. In the successive

deformation with route A, the pattern of stretch variation and the angular position of maximum and minimum stretches are the same for all passes. Moreover, as the number of the bimetallic samples passing through the ECAP die increased, the maximum stretch increased, but the minimum stretch is zero for all the passes. Considering the fact that the cold welding between constituents of core/shell bimetallic materials occurs only when the surface stretch exceeds a threshold value [4], it can be concluded that the cold welding between sheath and core of bimetallic materials can only be created by repetition ECAP process in the interface zones far from the angular position of the minimum stretch.

In contrast to route A, as Fig. 5 shows, the pattern of stretch for the even passes differed from odd passes in the ECAP process with route B_C. In the range of $0^o \langle \theta \le 90^o$, the angular position of minimum stretch is 90º for all passes, and the angular position of maximum stretch(θ_m) is always 45º in even passes. But the stretch curve is shifted to the right, as illustrated in Fig. 6a, and the value θ_m is increased from 0º to above 40º as the pass number increases in odd passes. In addition, by increasing the number of passes, both maximum
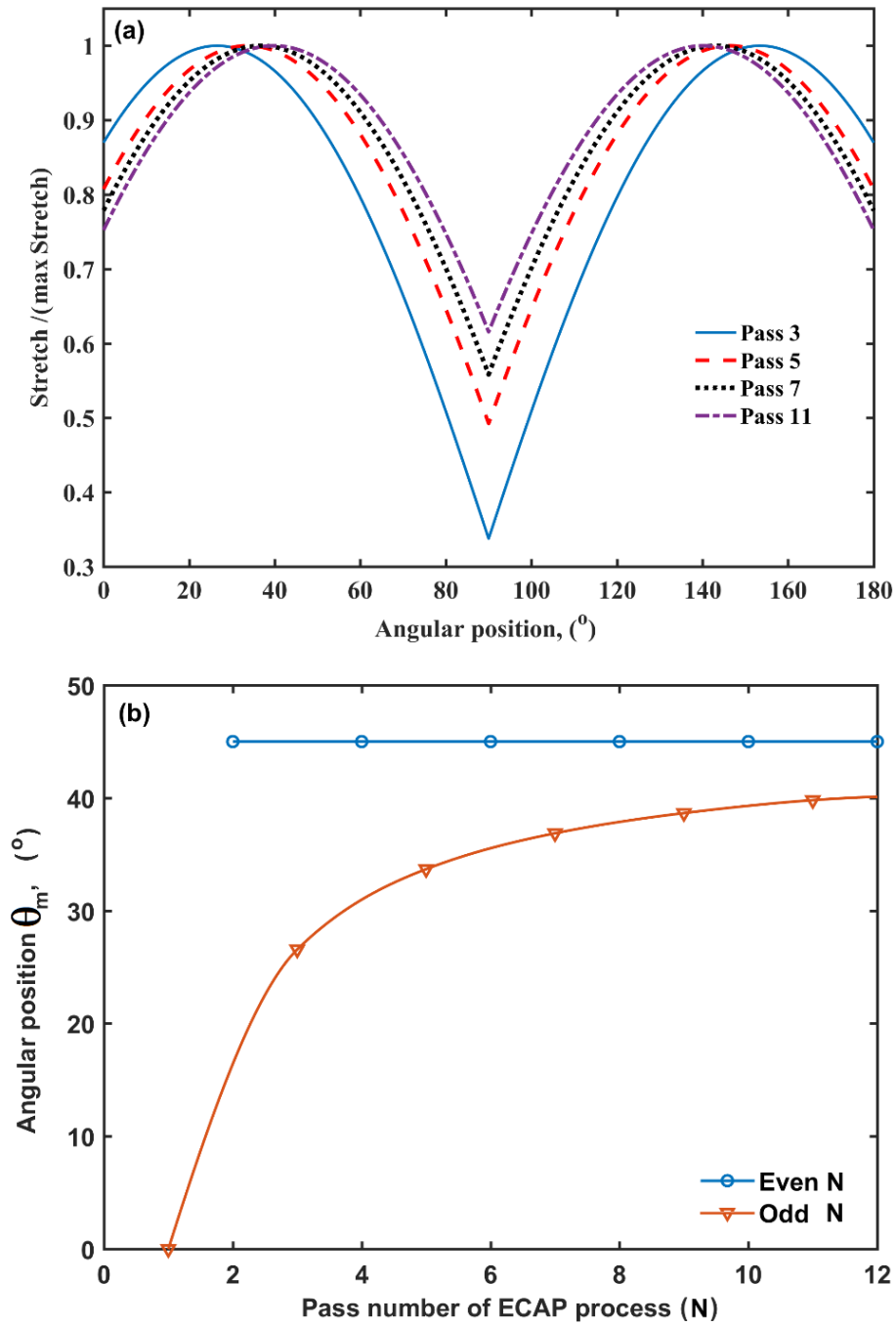
Fig. 6. The presentation of (a) shifting of stretch/(maximum stretch) ratio curve and (b) variation of the angular position of the maximum stretch( ) with the change of number pass deformation with route BC (φ=90º and ψ=30º)
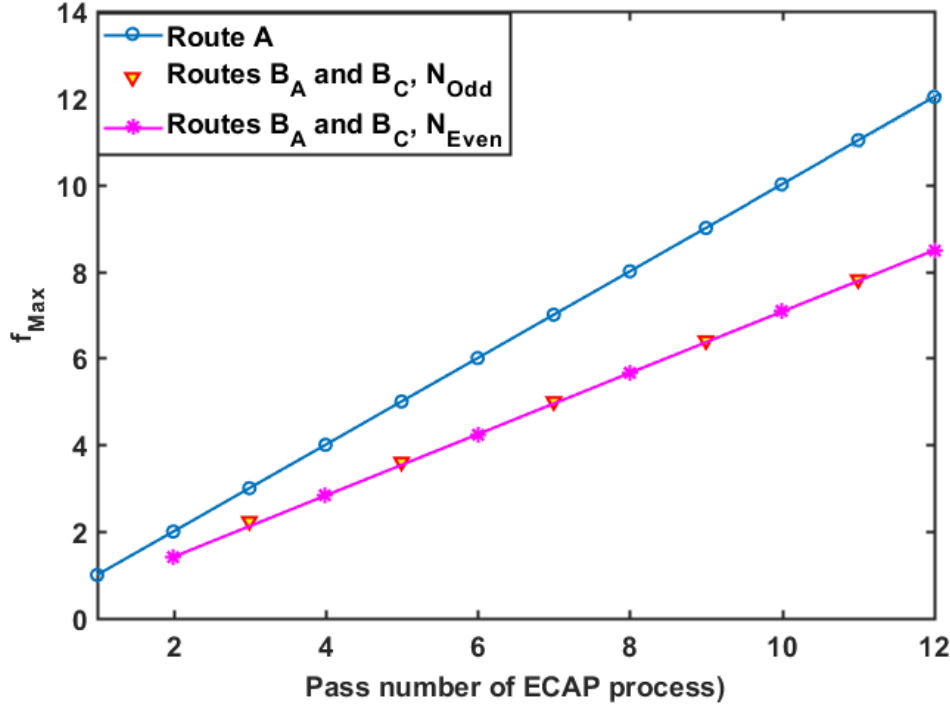
Fig. 7. The variation of the maximum coefficient of shear strain (f_{max}) with the odd and even number of deformation passes (N_{Odd} and N_{even}) with routes A, BA, and BC.

and minimum stretch values are increased. This means that the stretch value in all angular positions can be increased beyond the threshold value after several passes of deformation with route B, which satisfied the condition for cold welding occurrences and the formation of a wavy interface throughout the bimetallic sheath/core interface.

Since the angular position of maximum stretch (θ_m) in the range of θ_m is equal to 0° for all passes deformation with route A, the Eq. (8) can be reduced to the following form to calculate the value of maximum stretch-induced during N successive passing of sample through the ECAP die with route A:

$$St_{NA-\max} = 100 \times (\sqrt{1+(N.\gamma)^2} - 1) \qquad (10)$$

In the ECAP deformation with B_A and B_C routes, the angular position of maximum stretch in the range of $0^o \langle \theta \leq 90^o$ is changed in each pass (see Figs. 6a and 6b), and therefore it seems that there is no single relationship between the maximum stretch induced during N successive passage of the sample through the ECAP die with B_A and B_C routes($St_{NA-\max}$) and the values of γ. The angular position values corresponding to extreme values of stretch (θ_m) in the range of $0^o \langle \theta \leq 90^o$ can be obtained by setting the slope of the Eq. (7) to zero and then using these data, it can be investigated how the st_{NB_Max} is changed with the number of pass deformation (N).

Considering Eq. (9), the derivation of Eq. (7) leads to the $\theta_m = \text{Arctan}((N-1)/(N+1))$, when N is odd and $\theta_m = \pi/4$ when N is even. These relations indicated that the angular position corresponding to extreme stretch values is independent of the number of pass deformation with routes B_A and B_C, when N is even. Still, its value increased by increasing the number of pass deformation, when N is odd as sown in Fig 6b. By replacing the relations $\theta_m = \pi/4$, $\theta_m = \text{Arctan}((N-1)/(N+1))$ into Eq. (9) the coefficients of shear strain corresponding to extreme values of the stretch of the proposed routes for even $N(f_{Ev})$ and odd $N(f_{Od})$ are obtained as follows:

$$f_{Ev} = \frac{\sqrt{2}}{2}N \qquad (11)$$

$$f_{Od} = \frac{1}{2}[(|\cos(\theta_m)| + |\sin(\theta_m)|)N + (|\cos(\theta_m)| - |\sin(\theta_m)|)] \qquad (12)$$

Eq. (12) indicates that the maximum shear strain coefficient can be considered a linear function of pass number in the form of $f_{Od} = mN + c$, as shown in Fig. 7. The $m = (|\cos(\theta_m)| + |\sin(\theta_m)|)/2$ and $c = (|\cos(\theta_m)| - |\sin(\theta_m)|)/2$ are the line slope and intercept and their values for $3 \leq N \leq 20$ are

determined as 0.703 and 0.09 respectively. The percentage difference between the values predicted by Eqs. (11) and (12) is a function of N as follows:

$$\frac{f_{od} - f_{Ev}}{f_{Ev}} \times 100 =$$
$$\frac{0.703N + 0.09 - 0.7071N}{0.7071N} \times 100 \approx \frac{12.7}{N} - 0.6 \tag{13}$$

Eq. (13) indicates that the percentage difference between the values predicted by Eqs. (11) and (12) is less than 3.7% for $N \geq 3$. So, regardless of whether N is odd or even, Eq. (11) can estimate the shear strain coefficient in the ECAP deformation with B_A and B_C routes.

Finally, by placing Eq. (11) into Eq. (7), the relationship between St_{NB_Max} with shear strain and pass number can be determined as follows:

$$St_{NB\_Max} = 100 \times \left(\sqrt{1 + \frac{1}{2}(N\gamma)^2} - 1\right) \tag{14}$$

Considering the Eqs. (10) and (14), the St_{N_Max} can be expressed in the general form as follows:

$$St_{N\_Max} = 100 \times \left(\sqrt{1 + (mN\gamma)^2} - 1\right) \tag{15}$$

where the term $(mN\gamma)$ represents the total shear strain induced during N passes and m is 1 for routes A and C and is $\frac{1}{2}$ for routes B_A and B_C. The equivalent strain, $\varepsilon_{eq,1}$, induced during one cycle deformation is related to shear strain, γ, as $\gamma = \sqrt{3}\varepsilon_{eq,1}$ [19, 25]. So it can be written $mN\gamma = \sqrt{3}mN\varepsilon_{eq,1} = \sqrt{3}\varepsilon_{eq}$, where, $\varepsilon_{eq} = mN\varepsilon_{eq,1}$ represents the equivalent strain after N cycle deformation. On the other hand, according to Hollomon's relation, the flow stress σ_y after deformation corresponding to ε_{eq} is related to ε_{eq} and $N\gamma$ as:

$$\sigma_y = (k\varepsilon_{eq})^n = (kmN\gamma / \sqrt{3})^n \tag{16}$$

where the k and n are material constants. Based on Eq. (15), it can be obtained:

$$mN\gamma = \sqrt{(10^{-2} St_{N\_Max} + 1)^2 - 1} \tag{17}$$

Hence, flow stress after N passes deformation with the ECAP process (Eq. (16)) may be expressed as a function of the maximum stretch as follows:

$$\sigma_y = k_1[(10^{-2} St_{N\_Max} + 1)^2 - 1]^p \tag{18}$$

where $p = n/2$ and $k_1 = (k/\sqrt{3})^n$. Eq. (18) can be rearranged in the logarithmic form as:

$$Log\sigma_y = Logk_1 + p.Log[(10^{-2} St_{N\_Max} + 1)^2 - 1] \tag{19}$$

According to Eq. (19), the relationship between $x = Log[(10^{-2} St_{N\_Max} + 1)^2 - 1]$ and $y = Log\sigma_y$ should be linear. Parameters needed to ensure the validity of this impression are the values of maximum stretch and flow stress of bimetallic samples after each passes deformation by the ECAP process. Thus, for conducting the evaluation, the values of maximum stretch-induced during the first, second, and third passes with routes B_C for ECAP die having $\phi=90^o$ and $\psi=30^o$ are calculated using Eq. (14). To determine the correspondent's values σ_y, tensile tests are performed on the specimens prepared from the steel core of bimetallic Cu/steel samples. The obtained engineering stress-strain curves are shown in Fig. 8. As can be observed, the ultimate strength of ECAPed samples is significantly (to three times) higher than those of the un-ECAPed sample. Grain refinement and changes in dislocation density can be attributed to this strengthening as ECAP progresses. While the specimen is pressed through the ECAP die, a severe shear strain is imposed. As a result, the dislocation density is drastically increased and the grains are severely refined [26]. As indicated in Ref [21], the grain size of steel core of copper/steel bimetal rod was reduced from the initial size of ~53 μm to ~19 μm after an applied third pass ECAP with route Bc. The dislocation density enhancing and grain refinement both cause high strain hardening. Thus, the strength of metals is considerably improved as subjected to the ECAP process [26].

The values of flow stresses of bimetallic Cu/steel samples (σ_{yB}) are determined as follows [27]:

$$\sigma_{yB} = V_{fs}\sigma_{ys} + (1 - V_{fs})\sigma_{yc} \tag{20}$$

where the $V_{fs} \approx 0.71$ is the volume fraction of steel core, σ_{yc} is flow stress of ECAPed steel core extracted from experimental stress-strain curves (after engineering stress converted into ones true), and σ_{yc} is the flow stress of ECAPed copper reported by Afsari and Ranaei [28]. Finally, using the obtained data, the variation of y versus x is plotted. The results are presented in Fig. 9. As observed, the variation of y versus x is revealed in excellent agreement with Eq. (19). Therefore, this equation, in conjunction
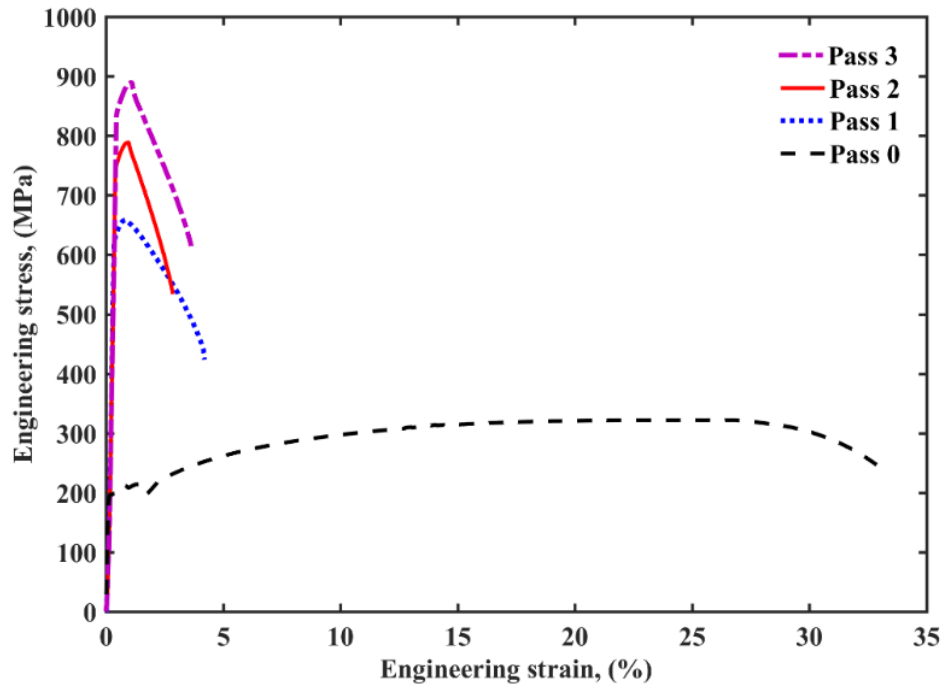
Fig. 8. Engineering tensile stress-strain curves for steel core of bimetallic samples before and after one, two, and three passes deformation by ECAP process.
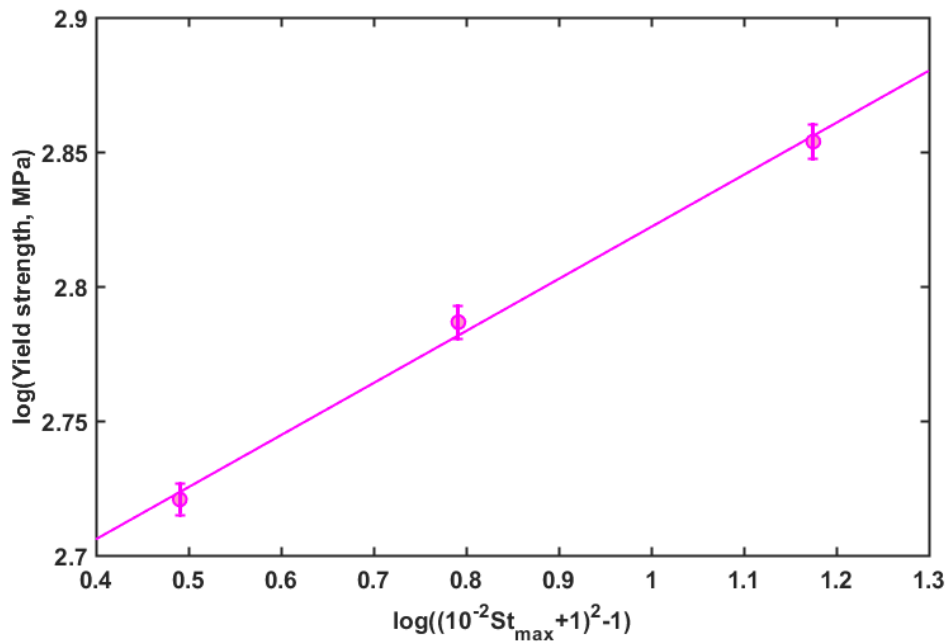

Fig. 9. The variation of $y = Log\sigma_y$ **versus** $x = Log[(10^{-2}St_{N\_Max} + 1)^2 - 1]$ **.**

with Eq. (15) can be used to estimate the yield strength of bimetallic samples after N passes deformation by ECAP process with a certain die.

5- Conclusions

In this research, considering the use of the ECAP process as a new method for the production of core/shell bimetal, as well as the key role of surface stretch in the formation of cold welding and wavy interfaces between the constituents of these materials, an attempt has been made to develop an analytical approach to account for the effect of repetitive passing of samples through dying with any deformation routes on the surface stretch-induced during ECAP process. The results indicated that obtaining completely cold welding throughout their interfaces is impossible between constituents of bimetallic samples even with several repeated ECAP processes with deformation route of A. A linear function is followed by the variation of the maximum induced stretch with pass numbers for a given die, with certain geometry. By increasing the number of pass deformations, the minimum stretch values and the angular position corresponding to extreme stretch values are increased in ECAP with routes B_A and B_C. Finally, excellent agreement is observed between the yield strength of ECAPed samples obtained from experimental stress-strain curves of copper/steel bimetallic samples and a new predictive model extracted from the general relationship between the maximum stretch, the passes numbers, and shear strain.

Acknowledgment

References

[1] A. Eivani, A.K. Taheri, A new method for producing bimetallic rods, Materials Letters, 61 (2007) 4110-4113.

[2] S. Ghadimi, M. Sedighi, F. Djavanroodi, A. Asgari, Experimental and numerical investigation of a Cu–Al bimetallic tube produced by ECAP, Materials and Manufacturing Processes, 30 (2015) 1256-1261.

[3] A.E. Medvedev, R. Lapovok, E. Koch, H.W. Höppel, M. Göken, Optimisation of interface formation by shear inclination: Example of aluminium-copper hybrid produced by ECAP with back-pressure, Materials & Design, 146 (2018) 142-151.

[4] M. Zebardast, A.K. Taheri, The cold welding of copper to aluminum using equal channel angular extrusion (ECAE) process, Journal of Materials Processing Technology, 211 (2011) 1034-1043.

[5] H. Mirzakouchakshirazi, A. Eivani, S. Kheirandish, Effect of post-deformation annealing treatment on interface properties and shear bond strength of Al-Cu bimetallic rods produced by equal channel angular pressing, Iranian Journal of Materials Science and Engineering, 14 (2017) 25-34.

[6] W. Hongyu, S. Jie, W. Zhenting, W. Qinglong, Z. Dewen, Z. Dianhua, Analysis of eccentric unbonded bimetal rod in ECAP based on different arrangements of soft and hard metals, Applied Mathematical Modelling, 47 (2017) 501-527.

[7] A.P. Zhilyaev, T. Werner, J.M. Cabrera, Characterization of Bimetallic Interface in Cu–Al and Ni–Cu Rods Cold Welded by Equal Channel Angular Pressing, Advanced Engineering Materials, 22 (2020) 1900653.

[8] N. Llorca-Isern, A.M. Escobar Romero, A. Roca, J.M. Cabrera, Equal channel angular pressing of Cu-Al bimetallic rod, in: Materials Science Forum, Trans Tech Publ, 2012, pp. 1811-1816.

[9] K. Narooei, A.K. Taheri, Strain field and extrusion load in ECAE process of bi-metal circular cross section, Applied Mathematical Modelling, 36 (2012) 2128-2141.

[10] Y. Qi, R. Lapovok, Y. Estrin, Microstructure and electrical conductivity of aluminium/steel bimetallic rods processed by severe plastic deformation, Journal of materials science, 51 (2016) 6860-6875.

[11] A. Eivani, S. Mirghasemi, S. Seyedein, J. Zhou, H. Jafarian, Simulation of deformation and fracture initiation during equal channel angular pressing of AZ31 magnesium alloy with covered tube casing, Journal of Materials Research and Technology, 12 (2021) 1913-1923.

[12] R. Jahadi, M. Sedighi, H. Jahed, Effects of aluminum and copper cover tube casing on the ECAP process of AM30 magnesium alloy, Materials and Manufacturing Processes, 32 (2017) 1375-1383.

[13] F. Djavanroodi, M. Daneshtalab, M. Ebrahimi, A novel technique to increase strain distribution homogeneity for ECAPed materials, Materials Science and Engineering: A, 535 (2012) 115-121.

[14] N. Bay, Mechanisms producing metallic bonds in cold welding, WELDING J., 62 (1983) 137.

[15] P. Wright, D. Snow, C. Tay, Interfacial conditions and bond strength in cold pressure welding by rolling, Metals Technology, 5 (1978) 24-31.

[16] J.W. Cave, J.D, The mechanism of cold pressure welding by rolling, J. Inst. Met., 101 (1973) 203-207.

[17] L. Vaidyanath, M. Nicholas, D. Milner, Pressure welding by rolling, British Welding Jour, 6 (1959) 13-28.

[18] W. Chen, W. He, Z. Chen, Z. Zhou, Q. Liu, Effect of wavy profile on the fabrication and mechanical properties of Al/Ti/Al composites prepared by rolling bonding: Experiments and finite element simulations, Advanced Engineering Materials, 21 (2019) 1900637.

[19] B.-W. Li, H.-P. Zhao, Q.-H. Qin, X.-Q. Feng, S.-W. Yu, Numerical study on the effects of hierarchical wavy interface morphology on fracture toughness, Computational Materials Science, 57 (2012) 14-22.

[20] J. Cui, G. Sun, G. Li, Z. Xu, P.K. Chu, Specific wave interface and its formation during magnetic pulse welding, Applied Physics Letters, 105 (2014) 221901.

[21] A. Rashidi, M. Etemadi, Investigation wavy interface forming and stretching in severe plastic deformed copper/steel bimetallic rod, Mechanics of Advanced Materials and Structures, (2020) 1-10.

[22] M. Howeyze, A. Eivani, H. Arabi, H. Jafarian, Effects

of deformation routes on the evolution of microstructure, texture and tensile properties of AA5052 aluminum alloy, Materials Science and Engineering: A, 732 (2018) 120-128.

[23] Q. Li, X. Jiao, Exploration of equal channel angular pressing routes for efficiently achieving ultrafine microstructure in magnesium, Materials Science and Engineering: A, 733 (2018) 179-189.

[24] A. Eivani, H. Mirzakoochakshirazi, H. Jafarian, Investigation of joint interface and cracking mechanism of thick cladding of copper on aluminum by equal channel angular pressing (ECAP), Journal of Materials Research and Technology, 9 (2020) 3394-3405.

[25] Y. Iwahashi, Z. Horita, M. Nemoto, J. Wang, T.G. Langdon, Principle of equal-channel angular pressing for the processing of ultra-fine grained materials, Scripta materialia, 35 (1996) 143-146.

[26] A. Gupta, B. Chandrasekhar, K.K. Saxena, Effect of Equal-channel angular pressing on mechanical Properties: An overview, Materials Today: Proceedings, (2021).

[27] M. Etemadi, A.M. Rashidi, Investigation of equal-channel angular pressing of steel/copper bimetallic rods and effect of Cu-shell thickness on imposed surface stretch, Modares Mechanical Engineering, 21 (2021) 79-89.

[28] A. Afsari, M. Ranaei, Equal channel angular pressing to produce ultrafine pure copper with excellent electrical and mechanical properties, International Journal of Nanoscience and Nanotechnology (IJNN), 10 (2014) 215-222.